

Direct Optical Measurement of Surface Dielectric Responses: Interrupted Growth on (001) GaAs

D. E. Aspnes,⁽¹⁾ Y. C. Chang,⁽²⁾ A. A. Studna,⁽¹⁾ L. T. Florez,⁽¹⁾ H. H. Farrell,⁽¹⁾ and J. P. Harbison⁽¹⁾

⁽¹⁾*Bellcore, Red Bank, New Jersey 07701-7040*

⁽²⁾*University of Illinois, Urbana, Illinois 61801*

(Received 31 July 1989)

Anisotropies of the visible-near-ultraviolet dielectric responses of various (001) GaAs molecular-beam-epitaxy surfaces are measured at temperature using a new optical double-modulation technique and a low-strain fused-quartz window. Tight-binding calculations identify structure at 1.8 eV with Ga dimers and at 2.6 and 4.1 eV with As dimers. Transient behavior on interruption of As flux is substantially altered by misorientation, suggesting substantially different *terrace* properties for vicinally cut surfaces.

PACS numbers: 68.55.Bd, 73.20.At, 78.65.Fa

We report the first direct optical measurement of a surface dielectric response, specifically the anisotropic part, obtained with a new double-modulation approach that avoids the usual need of optical studies to modify the surface and hence can be used under steady-state conditions and with buried interfaces. This realizes, at least in part, a goal that has been pursued for over 20 years,^{1,2} as dielectric responses give direct information about the fundamental excitations of surfaces and interfaces while the noninvasive, nondestructive nature of optical probes makes them ideal for use in a number of areas including real-time studies of crystal growth. We apply this new capability to gain a greater understanding of interrupted growth on (001) GaAs by molecular-beam epitaxy (MBE), a process that has assumed new importance as growth interruptions appear to be essential for preparing vertical superlattices.³⁻⁶ We observe prominent peaks at 1.8, 2.6, and 4.1 eV in various surface reconstructions, and relate these by tight-binding calculations to optical transitions involving Ga surface-dimer to lone-pair states, As lone-pair to surface-dimer states, and As surface dimers, respectively. With these identifications, and by taking advantage of the energy-local nature of the imaginary part of the dielectric response, we follow the dynamic evolution of surface coverage by Ga dimers for the singular and two vicinal (001) orientations when the As flux is interrupted. The substantial dependence of transient behavior on misorientation shows that steps significantly modify local *terrace* properties as well.

As described previously,⁷⁻⁹ our basic approach takes advantage of the intrinsic symmetry of cubic materials by using polarization modulation to suppress the dominant (99%–99.99%) bulk component of the near-normal-incidence reflectance R and to enhance the weak (0.01%–1%) surface contribution. Modulation of the incident polarization by a 50-kHz photoelastic element generates signals at 50 and 100 kHz that yield the phase and amplitude, respectively, of the relative complex reflectance difference, $\Delta\tilde{r}/\tilde{r} = \Delta r/r + i\Delta\theta = (\tilde{r}_{110} - \tilde{r}_{\bar{1}10})/\tilde{r}$,

between the near-normal-incidence complex reflectances \tilde{r}_{110} and $\tilde{r}_{\bar{1}10}$ of light linearly polarized along the [110] and $[\bar{1}10]$ principal axes, respectively, of the (001) GaAs growth surface that we study here. The new feature is a simultaneous slow (~ 0.1 -Hz) rotation of the sample, which interchanges these axes twice per mechanical cycle and thereby simulates nondestructively, under steady-state conditions, the surface modifications previously needed to eliminate systematic errors. From the accurate values of $\Delta\tilde{r}/\tilde{r}$ thus obtained we determine $\Delta(\epsilon d)$, the surface dielectric anisotropy (SDA), as¹⁰

$$\Delta(\epsilon d) = (\epsilon_{110} - \epsilon_{\bar{1}10})d = i \frac{\lambda}{4\pi} (\epsilon_s - 1) \frac{\Delta\tilde{r}}{\tilde{r}},$$

where ϵ_s is the dielectric function of the bulk material and λ is the wavelength of light. Advantages of this double-modulation approach relative to previous work are comparable to those of spectroellipsometry relative to spectrophotometry: direct access to $\Delta(\epsilon_2 d)$, which being local in energy is a direct probe of the elementary excitations of the system; the capability of obtaining dielectric function data without Kramers-Kronig analysis; more stringent constraints on interpretation; and results obtained in a form that can be compared directly to theory, thereby allowing structure to be identified by comparison to model configurations that cannot be isolated experimentally.

Experimental details about the Varian Gen-II MBE station and the photoelastic-modulator RD spectrometer are given elsewhere.⁹ Also essential to these experiments is a low-strain fused-quartz window¹¹ that is nearly free of the inhomogeneous strain characteristic of conventional viewports and can be externally heated to remove growth deposits without having to vent the station. Double-modulation data were obtained either by rotating the sample or by sequentially incrementing its azimuth by 90°. By carefully calibrating¹⁰ the $\Delta\theta$ and $\Delta r/r$ signals we obtain $\Delta\tilde{r}/\tilde{r}$ to 5% accuracy, which is better than that related to duplicating growth conditions in an MBE chamber.

Figure 1 summarizes $\Delta(\epsilon_2 d)$ spectra for various reconstructions on singular (001) GaAs, an orientation hereafter denoted by S . The 481°C ϵ_s data of Lautenschlager *et al.*¹² were used in the analysis. From fine structure in reflection high-energy electron diffraction (RHEED) patterns,¹³ S is known to exhibit three distinct reconstructions, α , β , and γ , within the (2×4) symmetry class depending on As flux and sample temperature. The α and β reconstructions are dynamically stable at 580 and 510°C, respectively, under present growth conditions, allowing the corresponding SDA spectra to be obtained directly.

As the remaining reconstructions of Fig. 1 are unstable, their spectra had to be obtained indirectly. We first established a (2×4) reference surface, and then recorded the changes of $\Delta\bar{r}/\bar{r}$ at each measurement wavelength as the As flux was interrupted and the surface evolved to its Ga-saturated (4×2) limit. Representative $\Delta(\epsilon d)$ transients at 1.8 eV for S and for vicinal surfaces cut 6° off (001) toward (111) A and (111) B , hereinafter denoted as A and B , respectively, are shown in Fig. 2. We could then obtain SDA spectra at any time after As interruption by adding these changes to the known SDA spectrum of the (2×4) starting surface. Figure 1 shows five such SDA spectra for S , obtained at 1-s intervals from 1 to 5 s. The three final spectra, obtained 3, 4, and 5 s after As interruption, all correspond to surfaces showing a (4×2) RHEED pattern.

Figure 1 provides much greater insight into these growth surfaces than previously attainable. The broad 2.0–2.5-eV $\Delta R/R$ peak⁷ is now clearly separated into two structures: a positive $\Delta(\epsilon_2 d)$ peak at 1.8 eV associated with Ga-saturated (4×2) , and a negative $\Delta(\epsilon_2 d)$ peak at 2.6 eV associated with As-rich $(2 \times 4)\alpha$. Thus the ~ 2.0 -eV contribution to $\Delta R/R$ is caused by increasing absorption along $[110]$ that results from increasing Ga coverage, while the ~ 2.5 -eV contribution is caused

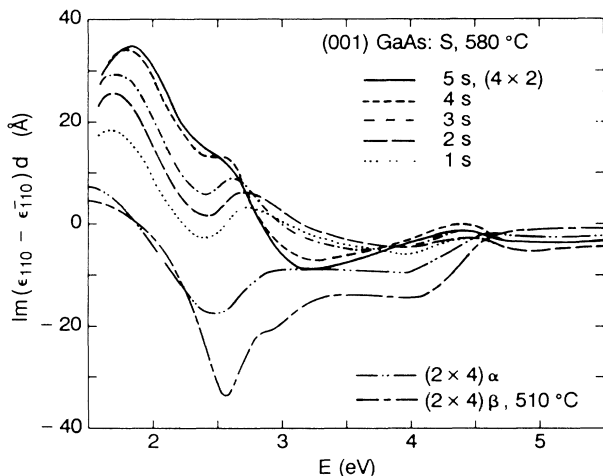


FIG. 1. Surface dielectric anisotropy spectra $\Delta(\epsilon_2 d)$ of various reconstructions on (001) GaAs.

by decreasing absorption along $[\bar{1}10]$ that results from decreasing As coverage. Both contributions appear positive in $\Delta R/R$ because of the 90° orientational difference between the Ga-Ga and As-As dimers. The 2.6-eV structure has almost disappeared in the SDA spectrum of Ga-saturated (4×2) , which is consistent with its expected 75% termination by Ga.^{13–15}

We identify the origins of these structures by calculating the SDA spectra of the As-terminated (2×1) and Ga-terminated (1×2) reconstructions of (001) GaAs using a tight-binding model with four sp^3 wave functions and two unoccupied d orbitals of symmetry $(x^2 + y^2)$ and $(2z^2 - x^2 - y^2)$. The actual (4×2) and (2×4) reconstructions differ from (1×2) and (2×1) only by missing every fourth dimer,^{13–15} and thus (1×2) and (2×1) should provide a good (and computationally tractable) approximation to the dielectric properties of the real surfaces. Interaction parameters were determined at 0 and 850 K by fitting calculated bulk ϵ_s spectra to spectroellipsometric data.¹² The use of unoccupied d orbitals is unconventional but necessary to obtain the proper energy dependences of the unoccupied conduction bands at the surface.¹⁶ Although earlier theoretical work interpreted SDA spectra of (110) surfaces as a many-body phenomenon,^{17,18} recent work by Manghi *et al.*¹⁹ suggests that surface anisotropies of clean surfaces can be treated adequately in the one-electron approximation. Comparison of calculated and bulk ϵ_s spectra shows the calculation to be reliable to about 4 eV but to break down at higher energies.

The calculated (2×1) SDA spectrum is compared to

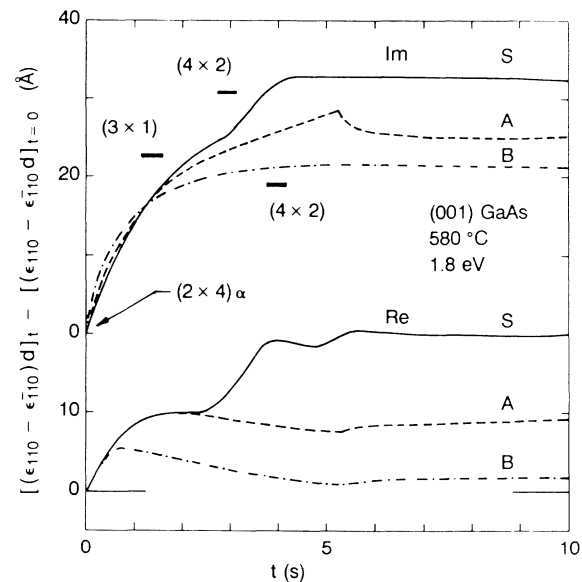


FIG. 2. Changes in the real and imaginary parts of $\Delta(\epsilon d)$ that occur for a singular (001) GaAs surface S and for two vicinal GaAs surfaces A and B cut 6° off (001) toward (111) A and (111) B , respectively. The onsets of various RHEED reconstruction patterns are also shown.

the measured $(2 \times 4)\beta$ spectrum at the top of Fig. 3. The calculated response is shown reduced by 25% to simulate the effect of the missing dimers. The measured peaks at 2.6 and 4.1 eV clearly correspond to the calculated peaks at 2.8 and 4.0 eV, which arise from transitions between filled As lone-pair states and the unoccupied As-As dimer antibonding orbital ($l-d^*$) and from transitions between As-As dimer bonding and antibonding orbitals ($d-d^*$), respectively. The background response in the calculations is caused by a continuum of transitions between filled backbonding levels and empty antibonding dimer orbitals. The calculated $l-d^*$ feature is larger than the measured peak but the agreement is satisfactory considering that the $(2 \times 4)\beta$ and (2×1) surfaces are not identical and that the surface contribution was calculated with no adjustable parameters. However, the measured and calculated amplitudes of the $d-d^*$ peaks are substantially different, and further work is needed to resolve this discrepancy. The $l-d^*$ identification together with the data of Fig. 1 show that the higher-temperature $(2 \times 4)\alpha$ reconstruction has about half as many As-As dimers as the $(2 \times 4)\beta$ phase, which is consistent with microscopic models^{13,14} and with the expected decrease of surface As at higher temperatures as a result of evaporation.

Similar calculations for Ga-terminated (1×2) reveal that the 1.8-eV structure is due to transitions between bonding Ga dimer orbitals and empty Ga lone-pair states ($d-l^*$). Again, the amplitude agreement at 1.8 eV is satisfactory. However, the measured and calculated spec-

tra are different at 4 eV, where the backbonding structures ($b-b^*$, $b-l^*$) are not seen in the data. Again, further work is needed to resolve this discrepancy.

With these identifications we return to the transient data of Fig. 2. As seen in Fig. 1, 1.8 eV coincidentally not only maximizes the sensitivity of $\Delta(\epsilon_2 d)$ to Ga-Ga dimers but also minimizes its sensitivity to the (2×4) reconstructions. The converse (not shown) is true for $\Delta(\epsilon_1 d)$. Thus, 1.8 eV is the natural choice for tracking the surface concentrations of both Ga-Ga and As-As dimers under interrupted-growth conditions. The data of Fig. 2, which are taken at this energy, are remarkable for their structural richness, which records the passage of these surfaces through various phases as they evolve from their As-rich starting condition to their Ga-rich ending condition. The data are also remarkable for their nonlinear time dependences, which show that Ga enrichment occurs not only by Ga deposition but also by As evaporation.²⁰

On all three surfaces, the most rapid process on As interruption is the nearly exponential transient with a time constant of 1 s or less seen only in $\Delta(\epsilon_1 d)$. The generality, time dependences, and virtual absence of this feature in $\Delta(\epsilon_2 d)$ identify this process as the evaporative loss of As-As dimers that are maintained in dynamic equilibrium with the surface when the As shutter is open.

The slower, smoother time dependences seen in $\Delta(\epsilon_2 d)$ reflect the concurrent accumulation of Ga-Ga dimers. Under present growth conditions the Ga-Ga dimer concentration increases smoothly and monotonically to equilibrium saturation for B but behaves very differently for S and A . Near 3 s the uptake of Ga-Ga-dimers by S accelerates sharply for about $\frac{1}{4}$ ML until equilibrium saturation is reached near 4.3 s. While the $\Delta(\epsilon_2 d)$ data appear to show final equilibrium at this time, the $\Delta(\epsilon_1 d)$ response indicates that this surface continues to evolve to 5.5 s. The $\Delta(\epsilon d)$ data for A show remarkable behavior, evolving smoothly to about 5.3 s and then breaking sharply to return to values previously observed near 4 s. We interpret this as a supersaturation phase transition involving the formation of metallic Ga droplets, which nucleate to provide an alternative sink for Ga when a critical excess surface concentration has been reached. Although not seen here, B also exhibits a similar response at lower As growth fluences.

The times at which the various RHEED reconstructions appear are also shown in Fig. 1. The starting configurations for A and S are (2×4) , while that for B does not show a well-defined superstructure along $[\bar{1}10]$. S converts to a threefold pattern along $[110]$ near 1.5 s and a fourfold pattern near 3 s. The rapid accumulation of Ga dimers for S between 3 and 4.3 s takes place within the (4×2) pattern, indicating that this uptake is a local structural modification filling remaining available sites. In contrast to S , A does not yield a fourfold reconstruction along $[110]$ at any time, indicating that under

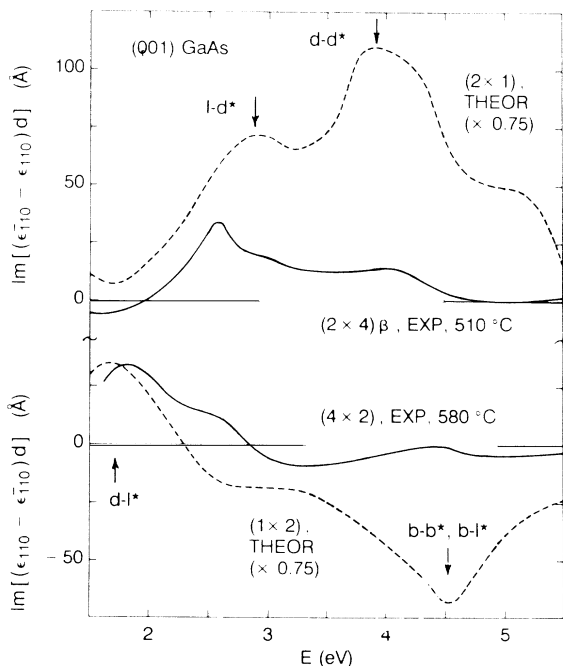


FIG. 3. Comparison of measured and calculated SDA spectra for (001) GaAs. For details see text.

these conditions the misorientation prevents the associated long-range order from occurring. The greater detail provided by the SDA transients, specifically the differences between S and A , shows that the well-known suppression of higher-order reconstruction patterns by steps on vicinal surfaces²¹ is not due entirely to the inability of a pattern to replicate across narrow terraces but involves local composition and structure as well.

The present results suggest numerous opportunities for further study. In the context of MBE, the sensitivity of growth surfaces to growth conditions implies that the present data represent only one of several possible outcomes of this experiment. In a broader context, identification of specific features in SDA spectra by a combination of theory and experiment provides new opportunities for kinetic studies as well as providing a surface-measurement alternative with diagnostic power complementary and comparable to RHEED, of particular interest for growth environments such as organometallic chemical-vapor deposition where RHEED cannot be used. In an even broader context, the present approach will be useful for studying a wide variety of interfaces as well as surfaces involving crystalline materials, examples that include but are not necessarily limited to etching, gas- and liquid-solid interactions, and semiconductor-oxide and -metal interfaces.

¹A. Cricenti, S. Selci, F. Ciccacci, A. C. Felici, C. Goletti, Z. Yong, and G. Chiarotti, *Phys. Scr.* **38**, 199 (1988).

²G. Chiarotti, G. Del Signore, and S. Nannarone, *Phys. Rev. Lett.* **21**, 1170 (1968).

³J. M. Gaines, P. M. Petroff, H. Kroemer, R. J. Simes, R. S. Geels, and J. H. English, *J. Vac. Sci. Technol. B* **6**, 1378 (1988).

⁴M. Tsuchiya, J. M. Gaines, R. H. Yan, R. J. Simes, P. O. Holtz, L. A. Coldren, and P. M. Petroff, *Phys. Rev. Lett.* **62**, 466 (1989).

⁵T. Fukui and H. Saito, *Appl. Phys. Lett.* **50**, 824 (1987).

⁶T. Fukui and H. Saito, *J. Vac. Sci. Technol. B* **6**, 1373 (1988).

⁷D. E. Aspnes and A. A. Studna, *Phys. Rev. Lett.* **54**, 1956 (1985).

⁸D. E. Aspnes, J. P. Harbison, A. A. Studna, and L. T. Florez, *Phys. Rev. Lett.* **59**, 1687 (1987).

⁹D. E. Aspnes, J. P. Harbison, A. A. Studna, and L. T. Florez, *J. Vac. Sci. Technol. A* **6**, 1327 (1988).

¹⁰D. E. Aspnes, A. A. Studna, L. T. Florez, Y. C. Chang, J. P. Harbison, M. K. Kelly, and H. H. Farrell, *J. Vac. Sci. Technol.* **7**, 901 (1989).

¹¹A. A. Studna, D. E. Aspnes, L. T. Florez, J. P. Harbison, and R. Ryan, *J. Vac. Sci. Technol. A* **7** (to be published).

¹²P. Lautenschlager, M. Garriga, S. Logothetidis, and M. Cardona, *Phys. Rev. B* **35**, 9174 (1987).

¹³H. H. Farrell and C. L. Palmstrøm (to be published).

¹⁴H. H. Farrell, J. P. Harbison, and L. D. Peterson, *J. Vac. Sci. Technol. B* **5**, 1482 (1987).

¹⁵D. J. Chadi, *J. Vac. Sci. Technol. A* **5**, 834 (1987).

¹⁶Y. C. Chang and D. E. Aspnes (to be published).

¹⁷W. L. Mochán and R. G. Barrera, *Phys. Rev. Lett.* **55**, 1192 (1985).

¹⁸D. E. Aspnes, *J. Vac. Sci. Technol.* **3**, 1498 (1985).

¹⁹F. Manghi, E. Molinari, R. Del Sole, and A. Selloni, *Phys. Rev. B* **39**, 13005 (1989).

²⁰J. R. Arthur, Jr., *Surf. Sci.* **43**, 449 (1974).

²¹R. Kaplan, *Surf. Sci.* **93**, 145 (1980).